Modeling and control of a XY positioning table

Conference Paper · November 2016

DOI: 10.1109/INDUSCON.2016.7874585

5 authors, including:

Lucas Moreira
GIPSA-lab
12 PUBLICATIONS **9** CITATIONS
SEE PROFILE

Christian Dias
Universidade Federal de Campina Grande (UFCG)
1 PUBLICATION **0** CITATIONS
SEE PROFILE

Péricles Barros
Universidade Federal de Campina Grande (UFCG)
125 PUBLICATIONS **373** CITATIONS
SEE PROFILE

George Acioli Junior
Universidade Federal de Campina Grande (UFCG)
38 PUBLICATIONS **69** CITATIONS
SEE PROFILE

Modeling and control of a XY positioning table

Lucas J. da S. Moreira*, Christian C. Dias†, Rafael B. C. Lima*, Péricles R. Barros‡ and George Acioli Júnior‡
*Post-Graduate Program in Electrical Engineering - PPgEE - COPELE
†Graduate Program in Electrical Engineering - PGEE
‡Electrical Engineering Department - DEE
Federal University of Campina Grande - UFCG
58429-900, Campina Grande - PB – Brazil
Emails: lucas.moreira@ee.ufcg.edu.br, chisthian.dias@ee.ufcg.edu.br, rafael.lima@ee.ufcg.edu.br,
prbarros@dee.ufcg.edu.br, georgeacioli@dee.ufcg.edu.br

***Abstract*— This paper is about modeling and control of a XY positioning table. It is described the construction and instrumentation of a double axis positioning system. It is developed a general electromechanical model, followed by the identification of simplified models for control purposes. At last, it is proposed a PID control strategy, tuned by Internal Model Control (IMC) technique.**

I. Introduction

Positioning systems are crucial equipments in modern industrial automation. XY positioning tables are the foundation of many applications such as CNC milling machines, laser burners, 3D printers, pick and place machines, bridge cranes, etc. All those applications demand efficient and accurate linear displacement control.

The first step in classical control system analysis is to establish a mathematical model of the proposed plant [1]. This model can be obtained by theoretical or experimental approach. Physical models are commonly used for design purposes and to understand plant behavior in operation, but they tend to be overly complex. For control purposes, it makes more sense to use system identification tools to estimate approximate models. A complete review of fundamentals of system identification can be found in [2] [3].

Over the past years, many techniques were developed for position control in XY tables. Linear Quadratic Gaussian (LQG) and Proportional and Derivative (PD) are proposed in [4] for a robust response, Sliding Mode Control (SMC) is introduced in [5] for nonlinear systems and neural adaptive controllers in [6]. Nevertheless, the PID controller is still the most common control structure, found in the majority of industrial setups [7].

In this paper, it is described the development stages of a two axis positioning table system. It is shown a brief description of plant construction, design and implementation of a supervisory system, electromechanical modeling, and a simple identification and control project, using Internal Model Control (IMC) for PID tuning.

II. Plant Description

This system can be split in two parts for a better understanding, physical structure for hardware components detailing and a software for human-machine interface using a PC.

A. Physical Structure

The plant consists of a two-axis positioning system, referred as axis X and Y, which can be moved independently. The linear displacement of shaft is done by the rotation of a DC motor, which is connected to a gearbox reduction that turns a set of pulleys and synchronizing belt engaged on the shaft, promoting rotational motion to linear motion. On each axis, it is possible to perform a displacement of 380mm, with the platform displacement limits identified by strokes end switches. Fig. 1 illustrates the system.

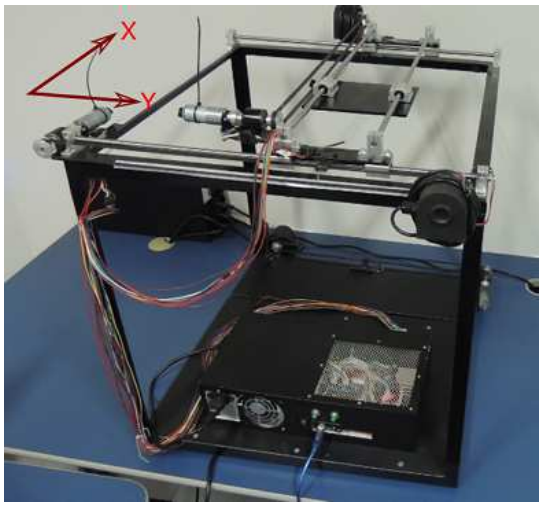

Fig. 1. Photo of XY positioning table

Both axis basically use the same set of electromechanical elements and sensors, as illustrated in Fig. 2, the only difference is in their size. Electromechanical elements and sensors are connected to a microcontrolled board, that is connected via USB to the computer.

1) DC motor with encoder: This DC motor consists of a low-power model with 6 VDC nominal voltage and an attached gearbox, with (78.83: 1) reduction ratio. There is also an integrated encoder with resolution of 48 pulses per turn, which provides 3591.84 pulses per revolution of the output shaft of the gearbox. The encoder, based on hall sensor, requires an input voltage between 3.5 and 20 VDC and consumes a

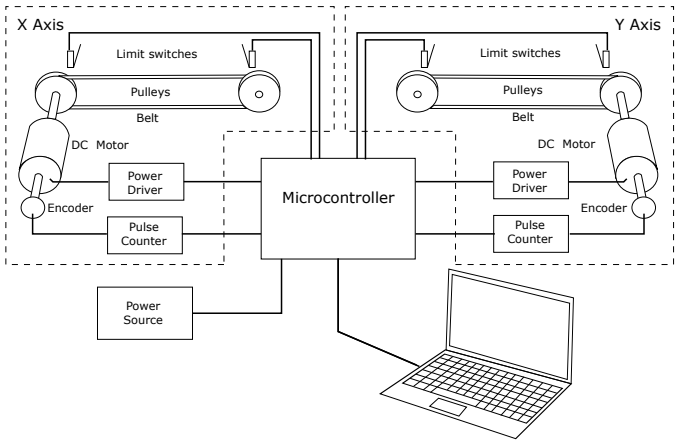

Fig. 2. Plant Schematic

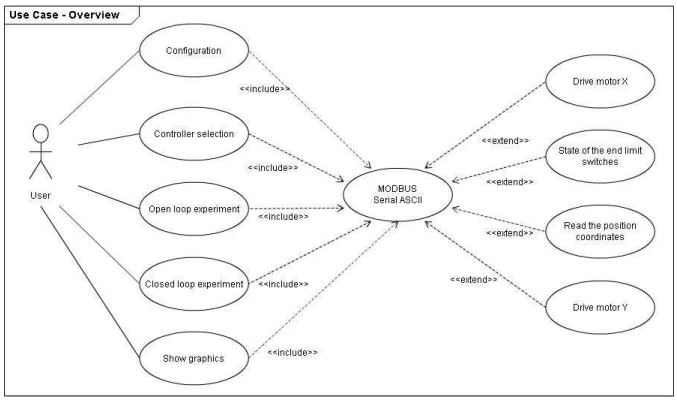

Fig. 3. Use case diagram

maximum current of 10 mA. The outputs A and B are square waves of DC to 0 VDC with approximately 90^o difference between them. Through monitoring of the levels of voltages at the outputs A and B, it is possible to determine motor speed and direction of rotation.

2) DC motor driver: For driving the DC motors, Dual VNH2SP30 Motor Driver Carrier MD03A module was chosen. This module performs control of two high-power motor, current up to 14A, by using an H-bridge, this can be used to reversing the direction of rotation by the module. Moreover, the power driver used in this module (VNH3SP30) allows the current triggered monitoring, providing an output voltage proportional to the current value, and also has overvoltage protection.

3) Pulse counter: The pulse counter chosen was the Dual LS7366R Quadrature Encoder Buffer module. This consists of two 32 bit counters, designed to interface directly to an encoder output, simplifying the total number of pulses monitoring task. SPI communication port is available to make the data exchange between the module and a microcontroller.

4) Microcontroller: Due to the popularization of development boards based on Arduino, it was decided that the microcontroller would be based on that platform, allowing future firmware changes without demanding high learning time. Thus, Arduino Mega model was selected due to its large number of GPIOs, compared with other Arduino platform boards.

B. Human Machine Interface Software

The XY platform program was developed to enable integration between the plant and the user, allowing to perform actions on the plant and monitor the effects of these actions on the intermediate charts. Fig. 3 illustrates the use case diagram with an overview of the operation of the program.

In the use case diagram, it is possible to realize various actions that can be performed by the user. They are detailed as following:

- Configuration - allows the selection of the serial communication port and communication speed, shift calibration and move the electromechanical assembly to the source;
- Controller selection - allows to select the type of controller that will act on the displacement of the electromechanical systems. The types of controllers provided: on-off, P, PI or PID;
- Open loop experiment - select the waveform of the excitation square wave or dual pulse, setting the time, amplitude and duty cycle of the pulse width in the case of excitation to be a double pulse;
- Closed loop experiment - similar options of the open loop, only in this case, the setting for the wave that served as a reference signal;
- MODBUS Serial ASCII – performs the communication between the software that is running on the computer and the firmware that is implemented in the Arduino Mega;
- Drive motor X or Y drive motor - these two actions are similar, the only difference being her acting shaft. This action is responsible for performing actions on/off the motor, reverse rotation and turn off the engine if the displacement limit is reached;
- State of the end limit switches - monitors the status of the end limit switches, informing the microcontroller when the displacement limit is reached;
- Read the position coordinates - performs functions related to the platform positioning, how to store the current position information and clearing the pulse counter.

The platform XY program interface was developed in MATLAB® computing environment, specifically the MATLAB GUI (Graphical User Interfaces). The GUI provides essential tools for creating user interfaces for custom applications and automatically generating MATLAB code to build the user interface, which can be adjusted to set the behavior of your application. GUI usually contains the controls such as menus, toolbars, buttons and sliders bars.

The implementation of use cases presented in Fig. 3 resulted in the system graphical interface shown in Fig. 4.

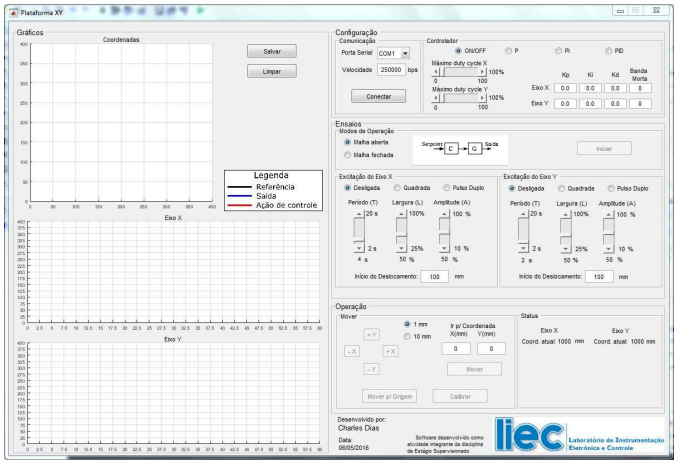

Fig. 4. Application Graphic Interface

III. Electromechanical Modeling

The XY positioning table is composed of two similar axis. But, for simplicity, it is modeled one axis at a time. The axis structure is further dismembered in two models, the actuator and belt-drive system. It is shown in Fig. 5 the electromechanical representation of its main components.

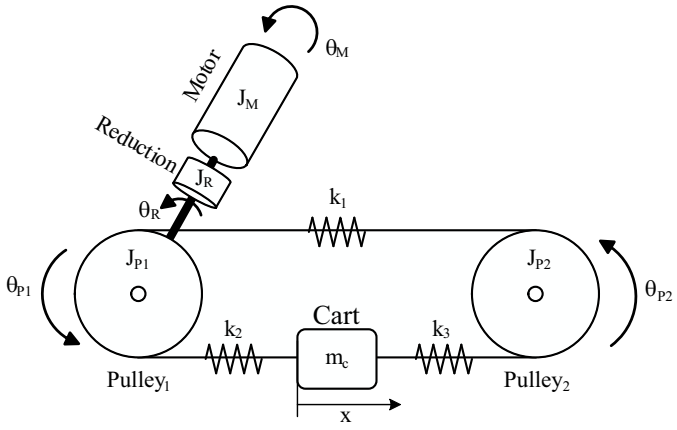

Fig. 5. One axis diagram

A. Actuator modeling

The actuator of each axis is an armature-controlled DC motor. Its electromagnetic schematic diagram is shown in Fig. 6.

The speed of an armature-controlled dc motor is controlled by the armature voltage e_a. For constant field current, the torque developed by the motor is

$$T_M = K_{M1} i_a \tag{1}$$

where K_{M1} is the motor torque constant and i_a is the armature current. When the armature is rotating, a voltage proportional to the product of the flux and angular velocity is induced in the armature. For a constant flux, the induced voltage e_b is

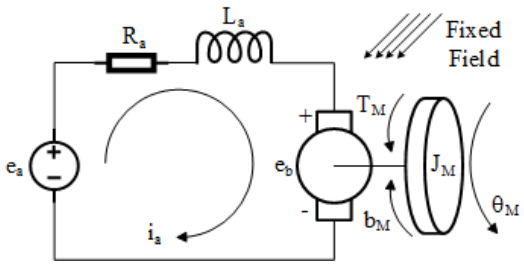

Fig. 6. DC motor electromagnetic diagram

directly proportional to the angular velocity

$$e_b = K_{M2} \frac{d\theta_M}{dt} \tag{2}$$

where e_b is the back emf, K_{M2} is the back emf constant of the motor, and θ_M is the angular displacement of the motor shaft.

By Kirchhoff's law, The differential equation for the armature circuit of Fig. 6 is

$$e_a = L_a \frac{di_a}{dt} + R_a i_a + e_b \tag{3}$$

$$= L_a \frac{di_a}{dt} + R_a i_a + K_{M2} \frac{d\theta_M}{dt} \tag{4}$$

The equation for torque equilibrium is

$$T_M = K_{M1} i_a = J_M \frac{d^2\theta_M}{dt^2} + b_M \frac{d\theta_M}{dt} \tag{5}$$

where J_M is the inertia and b_M is the viscous-friction coefficient of the the motor. By eliminating i_a and taking the Laplace transform of (3) and (5)

$$\frac{\theta_M(s)}{E_a(s)} = \frac{K_{M1}}{s(L_a s + R_a)(J_M s + b_M) + K_{M1} K_{M2}} \tag{6}$$

For small motors, the armature inductance can be neglected $L_a \ll R_a$ and the transfer function from armature voltage to motor shaft angular displacement is

$$\frac{\theta_M(s)}{E_a(s)} \approx \frac{K_{M1}}{s(R_a J_M s + R_a b_M + K_{M1} K_{M2})} \tag{7}$$

B. Belt-drive modeling

Each axis of the XY positioning table is driven by a belt and pulley system. The conversion of rotary to linear motion is affected by belt elasticity, pulley inertia, cart mass, friction etc. Using physical relations, it is possible to model the cart position, from motor angular displacement.

From Lagrange equation

$$\frac{d}{dt}\left(\frac{\partial L}{\partial \dot{q}_j}\right) - \frac{\partial L}{\partial q_j} = Q_j \tag{8}$$

where q_j is the generalized coordinate, $\dot{q}_j$ is the generalized velocity, Q_j are forces contributions and L is defined by (9)

$$L = E_c - E_p \tag{9}$$

E_c and E_p are kinetic and potential system energy. Neglecting potential energy, $E_p = 0$, (8) is re-written as

$$\frac{d}{dt}\left(\frac{\partial E_c}{\partial \dot{q}_j}\right) - \frac{\partial E_c}{\partial q_j} = Q_j \tag{10}$$

System kinetic energy is given by

$$E_c = \frac{m_M v_M^2}{2} + \frac{m_R v_R^2}{2} + \frac{m_{P1} v_{P1}^2}{2} + \frac{m_{P2} v_{P2}^2}{2} + \frac{m_c v_c^2}{2} \tag{11}$$

where m_j and v_j are mass and velocity of each j element. Considering all rotary elements as discs of radius r_j and mass m_j, inertia moment J_j is given by

$$J_j = m_j r_j^2 \tag{12}$$

or

$$m_j = \frac{J_j}{r_j^2} \tag{13}$$

The drive mechanism is constructed in such a way that the gearbox reduction ratio between motor angular displacement and pulley angular displacement is given by

$$n\theta_M = \theta_R = \theta_{P1} \tag{14}$$

angular velocity is related to angular displacement as

$$v_j = \dot{\theta}_j r_j \tag{15}$$

Replacing (13), (14), (15) and considering equal radius pulleys r

$$E_c = \frac{J_M \dot{\theta}_M^2}{2} + \frac{J_R \dot{\theta}_R^2}{2} + \frac{J_{P1} \dot{\theta}_{P1}^2}{2} + \frac{J_{P2} \dot{\theta}_{P2}^2}{2} + \frac{m_c v_c^2}{2} \tag{16}$$

$$E_c = (\frac{J_M + J_R/n^2 + J_{P1}/n^2}{2})\dot{\theta}_M^2 + \frac{J_{P2} \dot{\theta}_{P2}^2}{2} + \frac{m_c v_c^2}{2} \tag{17}$$

by grouping inertial moments of motor, reduction and pulley1

$$J_{eq} = J_M + J_R/n^2 + J_{P1}/n^2 \tag{18}$$

$$E_c = \frac{J_{eq} \dot{\theta}_M^2}{2} + \frac{J_{P2} \dot{\theta}_{P2}^2}{2} + \frac{m_c v_c^2}{2} \tag{19}$$

Replacing (19) in Lagrange (8) in which q_j is θ_M, θ_{P2} and x, with $\dot{x} = v_c$

$$J_{eq}\ddot{\theta}_M = T_M - \tau_{fM} \tag{20}$$

$$J_{P2}\ddot{\theta}_{P2} = r[K_2(x - r\theta_{P2}) - rK_3(\theta_{P2} - \theta_{P1})] - \tau_{fp2} \tag{21}$$

$$m_c\ddot{x} = K_1(r\theta_{P1} - x) - K_2(x - r\theta_{P2}) - \tau_{fx} \tag{22}$$

in which τ_{feq}, τ_{fp2} and τ_{fx} are friction torques.

The desired model, represented by the Equation system (20), (21) and (22), is very complex and nonlinear, but it can be significantly simplified depending on the accuracy of final application. A summary of main variables is shown Table I

Assuming that the friction torques present in all equations are constant and they can be classified as an additive disturbance in state estimation with the pulley position θ_{P1}. A possible linear solution for the Equation system (20), (21) and (22) is to re-write as State-Space form. The desired output are θ_M, θ_{P2}, x and the system input is the current applied in the DC motor i_a, that can be related to T_M by equation (1). Hence, the State-Space:

TABLE I

MAIN VARIABLES

Variable	Description	Unity
θ_M	Angular disp. of Motor	rad
θ_{P1}	Angular disp. of Pulley 1	rad
θ_{P2}	Angular disp. of Pulley 2	rad
θ_R	Angular disp. of Reduction	rad
x	Linear disp. of the cart	m
J_M	Inertia moment of motor	kgm^2
J_{P1}	Inertia moment of pulley 1	kgm^2
J_{P2}	Inertia moment of pulley 2	kgm^2
J_R	Inertia moment of reduction	kgm^2
b_M	Viscous-friction coef.	$kg/(ms)$
T_M	Torque of motor	kgm^2/s^2
τ_f	Friction torque	kgm^2/s^2
e_a	Armature voltage	V
e_b	Back emf voltage	V
i_a	Armature current	A
m_c	Mass of the cart	kg
n	Gearbox reducer ration	n/a
K_{M1}	Motor torque constant	Nm/A
K_{M2}	Back emf constant	Vs/rad
$K_{1,2,3}$	Elasticity coef. of belts	kg/s^2
R_a	Armature resistance	Ω
L_a	Armature inductance	H

$$\begin{bmatrix} \ddot{\theta}_M \\ \ddot{\theta}_{P2} \\ \ddot{x} \\ \dot{\theta}_M \\ \dot{\theta}_{P2} \\ \dot{x} \end{bmatrix} = \begin{bmatrix} 0 & 0 & 0 & 0 & 0 & 0 \\ 0 & 0 & 0 & 0 & -\frac{r^2(K_2+K_3)}{J_{P2}} & \frac{rK_2}{J_{P2}} \\ 0 & 0 & 0 & 0 & \frac{rK_2}{m_c} & -\frac{K_1+K_2}{m_c} \\ 1 & 0 & 0 & 0 & 0 & 0 \\ 0 & 1 & 0 & 0 & 0 & 0 \\ 0 & 0 & 1 & 0 & 0 & 0 \end{bmatrix} \begin{bmatrix} \dot{\theta}_M \\ \dot{\theta}_{P2} \\ \dot{x} \\ \theta_M \\ \theta_{P2} \\ x \end{bmatrix} + \begin{bmatrix} \frac{K_{M1}}{J_{eq}} \\ 0 \\ 0 \\ 0 \\ 0 \\ 0 \end{bmatrix} i_a - \begin{bmatrix} \frac{\tau_{fM}}{J_{eq}} \\ \frac{\tau_{fp2} - r^2K_3\theta_{P1}}{J_{P2}} \\ \frac{\tau_{fx} - rK_1\theta_{P1}}{m_c} \\ 0 \\ 0 \\ 0 \end{bmatrix} \tag{23}$$

$$\begin{bmatrix} \theta_M \\ \theta_{P2} \\ x \end{bmatrix} = \begin{bmatrix} 0 & 0 & 0 & 1 & 0 & 0 \\ 0 & 0 & 0 & 0 & 1 & 0 \\ 0 & 0 & 0 & 0 & 0 & 1 \end{bmatrix} \begin{bmatrix} \dot{\theta}_M \\ \dot{\theta}_{P2} \\ \dot{x} \\ \theta_M \\ \theta_{P2} \\ x \end{bmatrix} + \begin{bmatrix} 0 \\ 0 \\ 0 \\ 0 \\ 0 \\ 0 \end{bmatrix} i_a \tag{24}$$

IV. Experimental Results

In Section III, it was developed an nonlinear electromechanical model for one axis. In this Section, it is estimated a simplified model for control design. The proposed models are obtained by fitting experimental data using least squares method. Those models are used later for tuning PID controllers by IMC rules.

The Belt-drive dynamics were neglected, in experimental results, because of the absence of instrumentation in linear displacement measurements. Only angular displacement is available.

A. System Identification

In order to find a relationship between the input and output signals to the models obtained by (7), the transfer function for each set of motor and shaft have been identified. Aiming to extract the best results of system information with the available input signals, the double pulse was chosen. Then, the platform was set to the position (130,130) and the input signals with 15 seconds period, 50 mm amplitude and 6 second duty cycle were applied for both axis. The system behavior of these experiments are illustrated in Fig. 7 and 8.

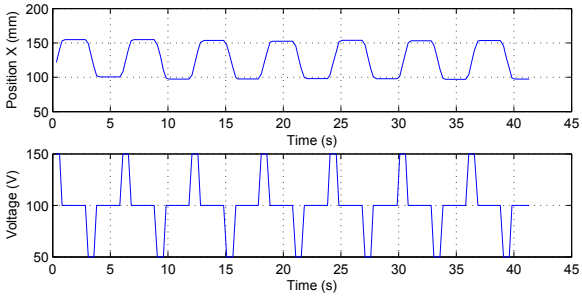

Fig. 7. Identification experiment for axis X

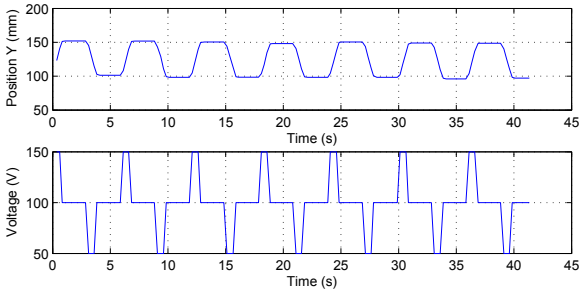

Fig. 8. Identification experiment for axis Y

From the collected data, continuous time transfer function models were identified in the MATLAB app *ident* [8]. According to the modeling section, the desired system should have two poles and one of those at the origin featuring an integrator. Based on these conditions, it was obtained the models:

$$G_x(s) = \frac{(1.345)}{s(1 + 0.01657s)} \tag{25}$$

$$G_y(s) = \frac{(1.336)}{s(1 + 1.0001x10^{-6}s)} \tag{26}$$

The models validations were computed by normalized mean square error criteria (NRMSE), described by (27), where y is real output value, $\hat{y}$ model output and $mean(y)$ the output mean. Those experimental models resulted in 87.02% and 84.30% fit for (25) and (26) respectively. Fig. 9 and 10 illustrate the comparison between experimental and simulated data, for the same initial conditions.

$$NRMSE = 100\left(1 - \frac{||y - \hat{y}||}{||y - mean(y)||}\right) \tag{27}$$

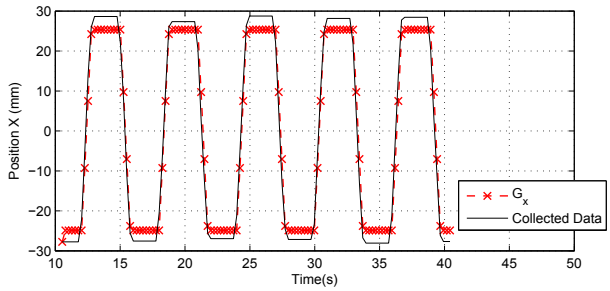

Fig. 9. Comparison of the identified model and the data collected for the X axis

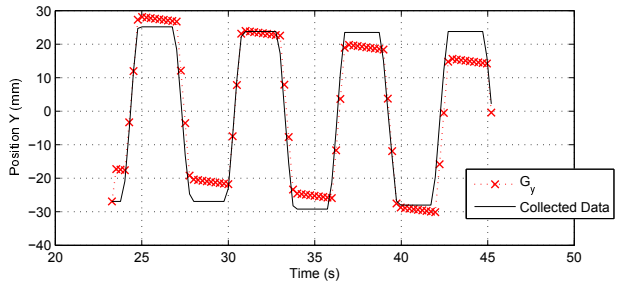

Fig. 10. Comparison of the identified model and the data collected for the Y axis

B. Control

Open loop operation is highly susceptible to plant variations and disturbances. It is proposed here a multivariable PID control strategy for robust closed loop operation.

Each PID is tuned using Internal Control Model technique (IMC) [9]. Open loop behavior is modeled by (25) and (26) and two PID controllers are tuned to match closed-loop dynamics represented by (28), where λ is an arbitrary time constant. Large λ implicates in slow and robust operation, while a smaller λ produces faster and less stable response. Hence, it was proposed two tests with different λ values, resulting in these parameters in the table II.

$$\hat{H}(s)\frac{2\lambda s + 1}{(2\lambda s + 1)^2} \tag{28}$$

TABLE II

PID CONTROLLER PARAMETERS

λ	**Model**	K_p	K_i	K_d
4.5	G_x	0.3311	0.0367	0.0055
4.5	G_y	0.3326	0.0370	3.326410×10^{-7}
7	G_x	0.2127	0.0152	0.0035
7	G_y	0.2138	0.0153	2.1384×10^{-7}

In order to evaluate the controllers performance, closed loop experiments were performed for each controller. The initial position was set to (250,250) and a square wave signal was applied with 20 mm amplitude and 10 seconds period. The results are illustrated in Fig. 11, 12, 13 and 14.

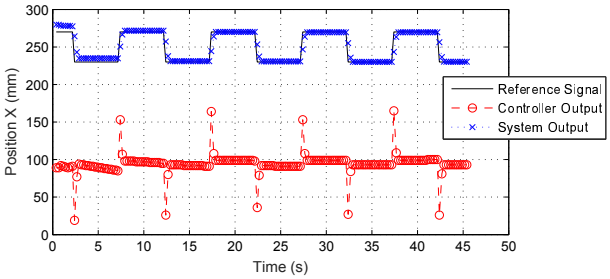

Fig. 11. Closed loop test, X axis, $\lambda = 4.5$

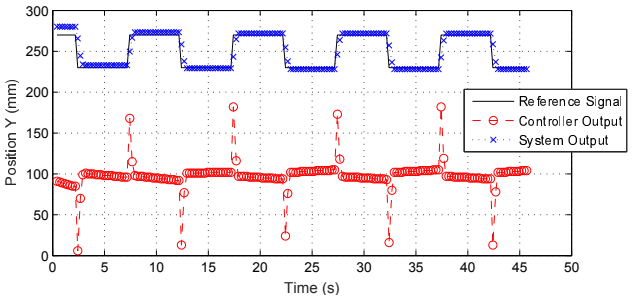

Fig. 12. Closed loop test, Y axis, $\lambda = 4.5$

By analyzing the experimental results, it is clear that for $\lambda = 4.5$ the system responded with little overshoot and fast convergence time. For $\lambda = 7$, the system behavior is not able to follow the reference, resulting in convergence erros in both axis. This is justified by the smoother response control action that is not able to overcome the viscosity and friction present in the plant. On the other hand, very quick responses would saturate the actuators, generating less robust systems, vulnerable to disturbance. Therefore, for IMC tuning technique, it is recommended values λ between 4.5 and 7.

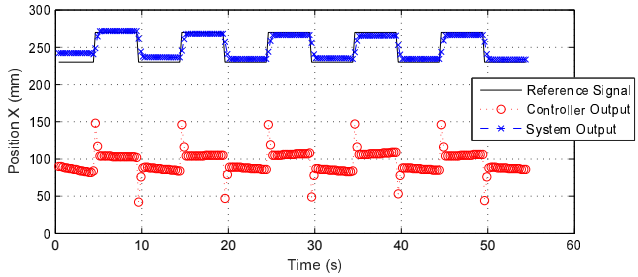

Fig. 13. Closed loop test, X axis, $\lambda = 7$

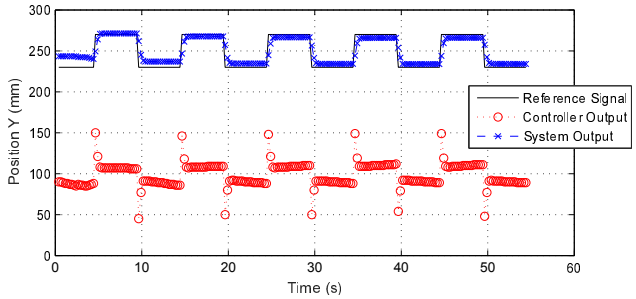

Fig. 14. Closed loop test, Y axis, $\lambda = 7$

V. CONCLUSION

It was shown in this paper, the main characteristics of a XY positioning table constructed by the authors. Details about plant instrumentation and human machine interface software, were presented. It was developed a non-linear dynamic model based on physical laws, that turns out to be overly complex for control purposes. Finally, it was estimated a data driven simplified model, that was employed in a IMC PID tuning strategy. In the end, two different tunings were compared, slow and robust versus fast and aggressive.

REFERENCES

[1] K. Ogata, *Modern Control Engineering*, 5th ed. New Jersey: Prentice-Hall, 2011.

[2] L. Ljung, *System Identification: Theory for the user*, 2nd ed. Prentice-Hall, New Jersey, 1999.

[3] T. Soderstrom and P. Stoica, *System Identification*, 1st ed. London: Prentice-Hall, 1989.

[4] J. R. L. Gomes, B. de Oliveira and P. Montenegro, "Técnicas de controle moderno aplicadas em uma mesa de coordenadas," *Rev. ciênc. exatas*, vol. 2, 2008.

[5] K. J. A. Hace and A. Sabanovic, "A new robust position control algorithm for a linear belt drive," *Proc. IEEE ICM*, pp. 329–334, 2004.

[6] B. S. d. O. J. B. de Menezes Filho, S. A. da Silva and J. A. Riul, "Controlador adaptivo neural para mesa de coordenadas x-y," *Rev. ciênc. exatas, Taubaté*, vol. 13.

[7] M. Campos and H. Teixeira, *Controles Típicos de Equipamentos e Processos Industriais*. Blucher, 2010.

[8] L. Ljung, *System identification toolbox*, The Matlab user's guide.

[9] M. M. D. E. Rivera and S. Skogestad, "Internal model control: 4. pid controller design," *Industrial and Engineering Chemistry Process Design and Development 25*, vol. 25, pp. 252–265, dez 1986.